Rolling Contact Fatigue Simulation Considering Surface Integrity

B. Zhang[1], G. Xiang[1], H. Liu[1*], P. Wei[1], J. Wu[1]

1 State Key Laboratory of Mechanical Transmissions, Chongqing University, China

Abstract
Rolling contact fatigue prediction is significant for the design of heavy-duty, high-reliability components, such as gears and bearings. For accurate prediction, it is vital to consider surface integrity parameters, such as surface roughness, hardness, and residual stress in the fatigue life model. Herein, an elastic-plastic finite element contact model of AISI 9310 rollers was developed, considering measured surface integrity parameters before and after shot peening. Subsequently, the Brown-Miller-Morrow multiaxial fatigue criterion was utilised to calculate fatigue life at each material point. By comparing with experimental results, the rolling contact fatigue model exhibits accurate simulation results and offers an effective tool for evaluating the effect of surface integrity on fatigue performance.

Keywords Rolling contact fatigue, shot peening, surface integrity, multiaxial fatigue

Introduction

As a primary failure mode of mechanical elements in aviation, wind turbines, ships, and automotive industries, rolling contact fatigue has become a crucial issue limiting operational reliability. Strengthening techniques enhance the anti-fatigue performance by altering various surface integrity parameters, including surface roughness, residual stress, hardness gradient, and material microstructure [1,2]. However, conducting fatigue tests uses large amounts of time and money. Furthermore, classical fatigue life model and parameters are difficult to meet strengthened components. Therefore, proposing an innovative rolling contact fatigue life model, which considers surface integrity parameters, is required.

The impact of one or two surface integrity parameters on contact fatigue has been well studied. W. Wang et al. [3] applied the Dang Van multiaxial fatigue criterion to discuss the evaluation of rolling contact fatigue of a carburised wind turbine gear, with consideration of residual stress and hardness gradient. L. Flour et al. [4] developed a numerical model to predict residual stress relaxation, and estimated the localisation of contact fatigue crack initiation, considering surface roughness. B. Zhang et al. [5] analysed the influence of surface roughness on fatigue and wear of an aviation gear, based on the Brown-Miller-Morrow multiaxial fatigue criterion and the continuous damage material constitutive behaviour. However, the contact fatigue behaviour under a complex combination of various surface integrity parameters has yet to be investigated. L. Cui et al. [6] established an elastic-plastic finite element fatigue damage accumulation model, which considered surface roughness, residual stress, and hardness of bearing rollers. Unfortunately, this model cannot be applied to surface-strengthened components, as gradient characteristics of hardness and residual stress induced by such surface engineering were not considered.

In this article, the surface topography, hardness gradient, and residual stress gradient of carburised rollers before and after shot peening were measured and applied in the finite element model. The kinematic hardening constitutive equation and the Brown-Miller-Morrow multiaxial fatigue criterion were employed to calculate the rolling contact fatigue life of each material point. Subsequently, rolling contact fatigue tests were conducted on a twin-disc rig. Experimental and simulation results were contrasted.

Experimental Method

Specimen: The specimen material is AISI 9310 steel with high surface hardness, which is widely utilised in the aerospace sector. Its chemical composition requirements are presented in Table 1. The specimens underwent rough turning, ultrasonic flaw detection, hardening, tempering, carburising, quenching, and grinding. The driving and driven specimens are illustrated in Figure 1.

Table 1. Chemical Compositions of AISI 9310.

C	0.07~0.13	Si	0.15~0.35
Mn	0.4~0.7	P	≤0.015
S	≤0.015	Cr	1.0~1.4
Mo	0.08~0.15	Ni	3~3.5
Cu	≤0.35	B	≤0.001

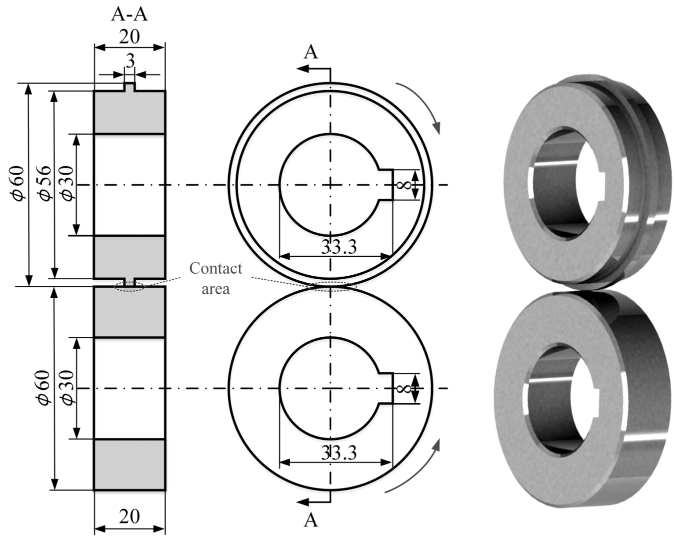

Figure 1. The Test Specimens.

Shot peening: The ground specimens were strengthened by the process of shot peening, using a pneumatic shot peening machine. Steel cut wire shot, with 0.6 mm diameter and 55~62 HRC average hardness, was adopted. The impact angle was 90°, and the diameter of the nozzle was 8 mm. The nozzle was maintained 150 mm away from the roller surface. The coverage rate reached 200% and shot peening reached 0.35 mmA.
Surface integrity test: The residual stress gradient, surface roughness, and microhardness gradient of specimens was measured, both before and after shot peening. The PULSTEC μ-360s portable residual stress detector was employed to measure residual stress at several depths. The surface micro-topography was measured using a white light interferometer. The average value of surface roughness was calculated following the removal of the curvature of rollers. The specimen microhardness was measured by a digital display automatic rotary microhardness tester (MHVS-1000AT). The loading force was 0.5 N and the load holding time was 10 seconds. The measurement results are displayed in Figure 2.
Rolling contact fatigue tests: Rolling contact fatigue tests were conducted for specimens before and after shot peening. A rolling contact fatigue testing machine (CQHH-RCF-A) was used for fatigue testing, which primarily consisted of the test system, the lubrication and cooling system, the control system, and the machine vision system. It can detect fatigue failure online through machine vision technology, enabling automatic shut-down. The rolling contact fatigue tester is illustrated in Figure 3. The contact stress was 2500 MPa (normal load of 2602 N), and the slip ratio was 10%. The driving speed was set at 1800 r/min, and the driven speed was 1980 r/min. The jetted lubricating oil was a commercial lubricant (Mobil 600 XP100).

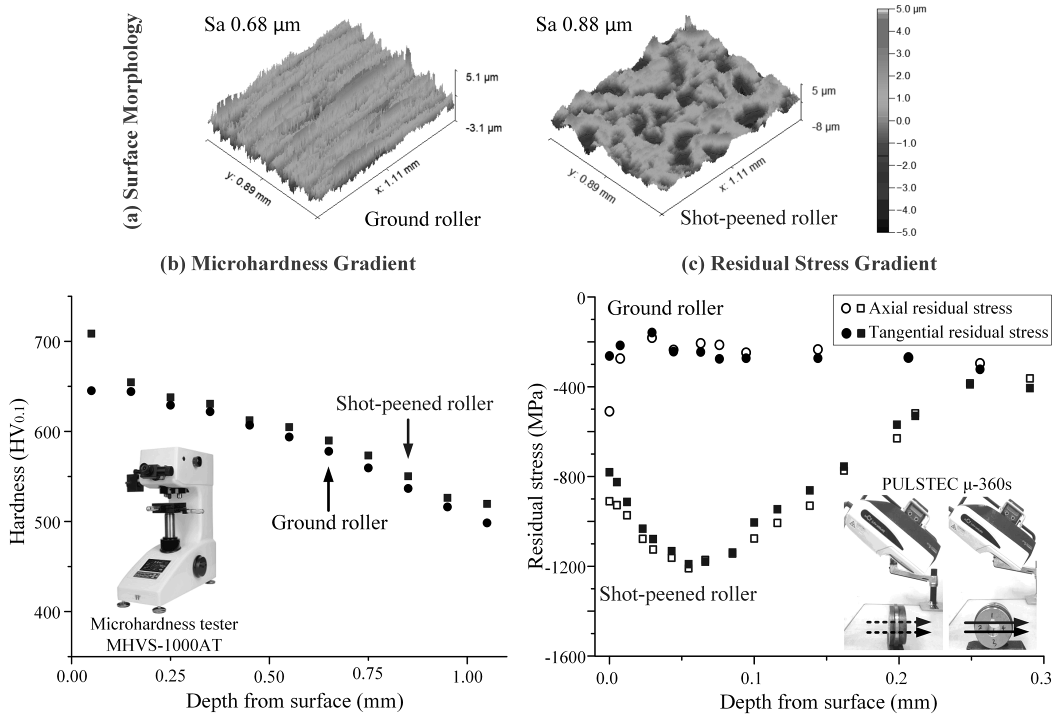

Figure 2. Measurements of Surface Integrity Parameters.

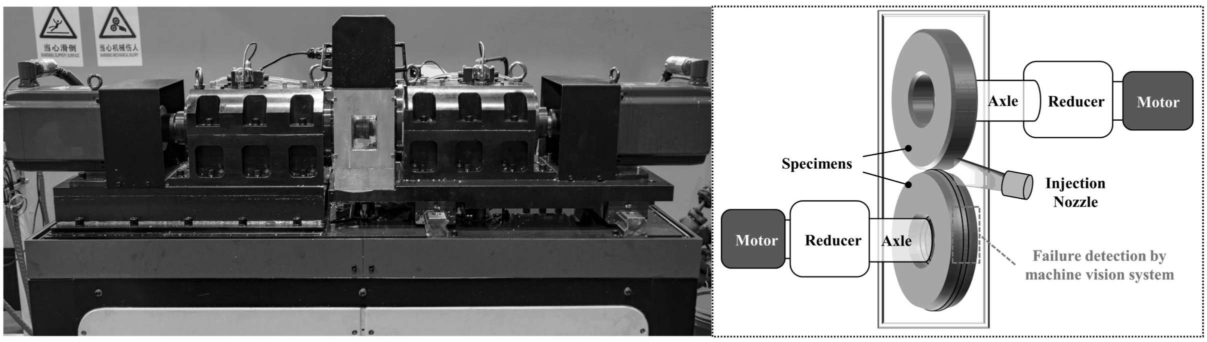

Figure 3. Rolling Contact Fatigue Tester.

Simulation Method

The elastic-plastic finite element model: The elastic-plastic finite element model of rollers was established, considering measured surface roughness, residual stress gradient, and hardness gradient. Following this, according to the stress-strain results, the fatigue life of the driving roller was calculated based on the Brown-Miller-Morrow fatigue life model. The modelling process of rolling contact fatigue is as follows:

1) Subsequent to removing the curvature of rollers, a rough curve was extracted along the tangential direction of the roller, which was further imported in the finite element model.

2) The finite element model was established in ABAQUS; the surface roughness was imported on the surface of the driving specimen by Python, and the surface of the driven specimen remained smooth.

3) Young's modulus E of specimens was 210 GPa, and the Poisson's ratio was 0.3. The kinematic hardening constitutive equation was applied, with the hardening modulus having been set to 10.5 GPa. The material yield strength was converted from measured hardness by the Pavlina-Tyne formula [7] as:

$$YS = -90.7 + 2.876HV \tag{1}$$

Where *YS* is the yield strength at a certain depth, and *HV* represents the measured hardness gradient.

4) The measured residual stress gradient was incorporated into the prestressed field.
5) The mesh size on the surface was 2 μm * 2 μm. The mesh size of the driven specimen was 0.5 mm * 0.5 mm.
6) A normal load of 2602 N was applied at the centre of the driven specimen. The coefficient of friction was assumed as 0.1, and the slip rate was 10%.
The elastic-plastic finite element contact model of AISI 9310 rollers is presented in Figure 4.

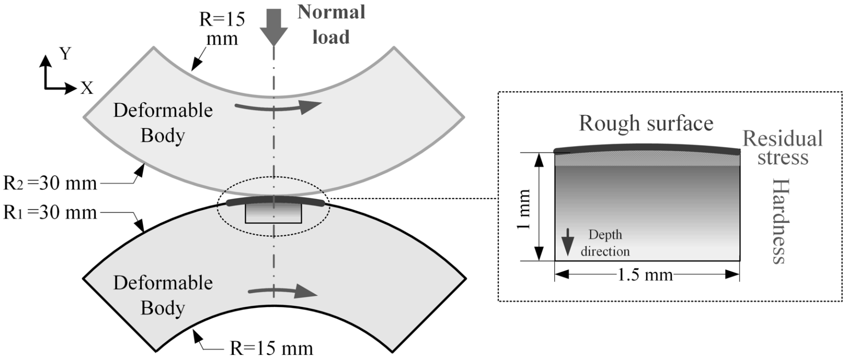

Figure 4. Elastic-plastic Finite Element Contact Model of AISI 9310 Rollers.

The Brown-Miller-Morrow fatigue life model: Considering the influence of surface roughness, residual stress, and hardness, plastic deformation may occur during the loading process, particularly at the near-surface area. Therefore, a strain-based multiaxial fatigue criterion was chosen. The Brown-Miller criterion assumes that the fatigue crack initiates along the plane with the maximum shear strain, before propagating along the normal strain direction on this plane. It is usual to define the plane with the maximum shear strain as the critical plane, on which the maximum shear strain and the normal strain are considered as damage variables. The Brown-Miller-Morrow fatigue life model [8] can be expressed as:

$$\frac{\Delta\gamma_{\max}}{2}+\frac{\Delta\varepsilon_n}{2}=1.65\frac{(\sigma_f^{'}-\sigma_m)}{E}(2N_f)^b+1.75\varepsilon_f^{'}(2N_f)^c \tag{2}$$

Where $\Delta\gamma_{\max}/2$ signifies the amplitude of the maximum shear strain, and $\Delta\varepsilon_{\mathrm{n}}/2$ and σ_m represent the normal strain amplitude and the mean stress on the critical plane, respectively. $\sigma_f^{'}$ and $\varepsilon_f^{'}$ denote the fatigue strength coefficient and the fatigue ductile coefficient, while b and c represent the fatigue strength exponent and the fatigue ductile exponent, respectively. $2N_f$ portrays the life of the material. In this work, the fatigue parameters were assumed as *b*=0.057, *c*=0.27, $\sigma_f^{'}=2894$, and $\varepsilon_f^{'}=0.134$.

As the critical plane at each material point is unknown, the shear strain, the normal strain, and the normal stress at each candidate plane should be calculated; subsequently, the plane with the maximum shear strain should be defined as the critical plane. The angle, θ, represents the angle of the critical plane to normal direction. The normal stress σ_θ, the normal strain ε_θ, and the shear strain γ_θ on each plane can be expressed as [9]:

$$\begin{cases}\sigma_\theta=\sigma_x\cos^2\theta+\sigma_z\sin^2\theta+2\tau_{xz}\sin\theta\cos\theta\\ \varepsilon_\theta=\varepsilon_x\cos^2\theta+\varepsilon_z\sin^2\theta+\gamma_{xy}\sin\theta\cos\theta\\ \gamma_\theta=\gamma_{xz}(\cos^2\theta-\sin^2\theta)+2(\varepsilon_z-\varepsilon_x)\sin\theta\cos\theta\end{cases} \tag{3}$$

The range of the maximum shear strain $\Delta\gamma_{max}$, the range of normal strain on the critical plane $\Delta\varepsilon_n$, and the mean normal stress σ_m on the critical plane can be expressed as:

$$\begin{cases} \Delta\gamma_{max} = \gamma_{max} - \gamma_{min} \\ \Delta\varepsilon_n = \varepsilon_{max} - \varepsilon_{min} \\ \sigma_m = \dfrac{\sigma_{max} + \sigma_{min}}{2} \end{cases} \tag{4}$$

Where γ_{max} and γ_{min} denote the maximum and minimum shear strain on the critical plane, respectively, ε_{max} and ε_{min} signify the maximum and minimum normal strain on the critical plane, respectively, and σ_{max} and σ_{min} represent the maximum and minimum normal stress on the critical plane, respectively.

Following the determination of the critical plane at each material point, the fatigue life at the corresponding material point can be iteratively calculated according to the Brown-Miller-Morrow fatigue life model.

Results and Discussion

Experimental results: Experimental data of rolling contact fatigue of AISI 9310 rollers, before and after shot peening, were processed following the two-parameter Weibull distribution. For rollers subjected to contact stress of 2500 MPa and slip ratio of 10%, test points and fitting curves are presented in Figure 5. The rolling contact fatigue life with 50% failure probability of ground rollers is 4,601,039, and fatigue life with 10% failure probability is 3,316,870. While the fatigue life under 50% and 10% failure probability of shot-peened rollers reach 5,861,465 and 3,922,395, respectively. It is evident that shot peening greatly heightens rolling contact fatigue life.

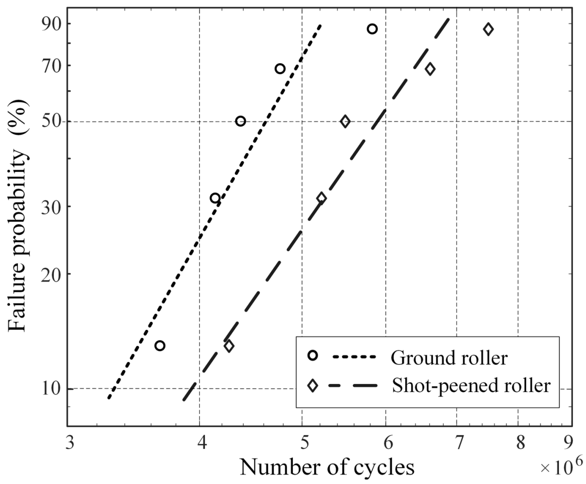

Figure 5. Experimental Results of AISI 9310 Rollers.

Simulation results: The simulated fatigue life of ground and shot-peened rollers are illustrated in Figure 6. Their minimum fatigue life occurs near the surface, and are 2,779,713 and 3,999,447, respectively. Compared to the 10% failure probability experimental results, the errors of simulated life before and after shot peening are 16.19% and 1.96%, respectively. This demonstrates that the proposed contact fatigue model enables an accurate prediction of rolling contact fatigue life. Due to the limited depth of residual stress introduced by shot peening, residual stress below the black dotted line is not considered. The fatigue life of material points above and below the dotted line is clearly different, which is evidence for the significance of residual compressive stress on fatigue life [3]. The reduction of fatigue life near the surface is shown in the red dotted circle, which is caused by surface roughness. It is generally accepted that, as surface roughness increases, the near-surface fatigue life decreases significantly [10]. Although surface roughness Sa of rollers is enhanced from 0.68 μm to 0.88 μm after shot peening, the hardness gradient and residual compressive stress layer are significantly heightened by shot peening. Thus, the near-surface material points are subject to complex combined impacts of surface integrity parameters.

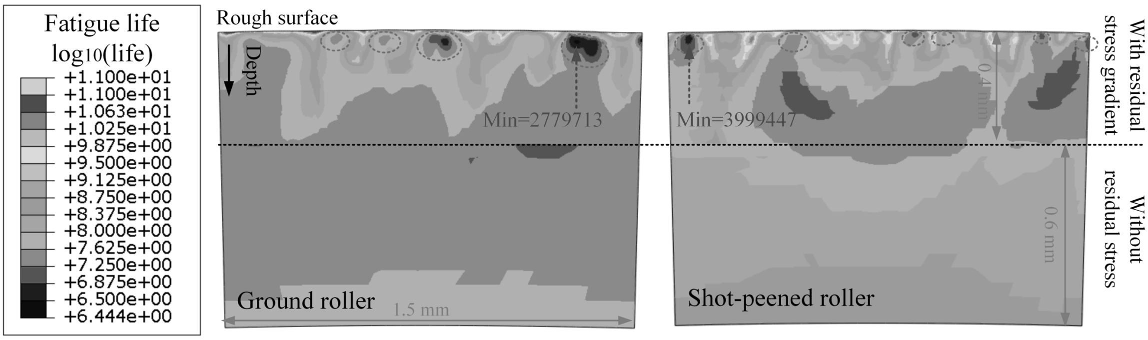

Figure 6. Simulation Results of AISI 9310 Rollers.

Conclusions

An elastic-plastic finite element rolling contact fatigue model of AISI 9310 rollers was established, considering measured surface integrity parameters before and after shot peening. By comparing findings with rolling contact fatigue tests, the proposed rolling contact fatigue model enables an accurate life prediction and provides an effective tool to evaluate the impact of surface integrity on contact fatigue life, with various manufacturing techniques. These techniques include shot peening, fine particle peening, superfinishing, and other surface treatments.

References

[1] I F Pariente, M Guagliano, *Influence of shot peening process on contact fatigue behavior of gears*. Materials and Manufacturing Processes, Vol. 24 (2009), pp 1436-1441.

[2] J Wu, H Liu, P Wei, et al., *Effect of shot peening coverage on residual stress and surface roughness of 18CrNiMo7-6 steel*. International Journal of Mechanical Sciences, Vol. 183 (2020), pp 105785.

[3] W Wang, H Liu, C Zhu, et al. *Evaluation of rolling contact fatigue of a carburized wind turbine gear considering the residual stress and hardness gradient*. Journal of Tribology, Vol. 140 (2018), pp 061401.

[4] L Flour. *Contact fatigue of automotive gears: evolution and effects of residual stresses introduced by surface treatments*. Fatigue & Fracture of Engineering Materials & Structures, Vol. 23 (2000), pp 217-228.

[5] B Zhang, H Liu, C Zhu, et al., *Simulation of the fatigue-wear coupling mechanism of an aviation gear*. Friction, Vol. 9 (2021), pp. 1616-1634.

[6] L Cui, Y Su. *Contact fatigue life prediction of rolling bearing considering machined surface integrity*. Industrial Lubrication and Tribology, Vol. 72 (2022), pp 73-80.

[7] E J Pavlina, C J V Tyne. *Correlation of Yield Strength and Tensile Strength with Hardness for Steels*. Journal of Materials Engineering & Performance, Vol. 17 (2008), pp 888-893.

[8] J D Morrow. *Cyclic plastic strain energy and fatigue of metals*. Internal Friction, Damping, and Cyclic Plasticity, (1965), pp 45-87.

[9] S. P. Timoshenko, J. N. Goodier, and H. N. Abramson, Theory of elasticity (3rd ed.). New York: NY: McGraw-Hill, 1970.

[10] B Zhang, H Liu, C Zhu, et al. *Numerical simulation of competing mechanism between pitting and micro-pitting of a wind turbine gear considering surface roughness*. Engineering Failure Analysis, Vol. 104 (2019), pp 1-12.